

Distinct Nuclear and Cytoplasmic Localization of Caspase Cleavage Products in Two Models of Induced Apoptotic Death in Dopamine Neurons of the Substantia Nigra

Tinmarla F. Oo,* Robert Siman,† and Robert E. Burke*^{‡,1}

*Department of Neurology and †Department of Pathology, The College of Physicians and Surgeons, Columbia University, New York, New York 10032; and ‡Department of Pharmacology, University of Pennsylvania School of Medicine, Philadelphia, Pennsylvania 19104

Received September 12, 2001; accepted January 26, 2002

An emerging theme in programmed cell death (PCD) of neurons is that the mechanisms involved depend on the cellular context and the death-inducing stimulus. One particular class of neurons for which it is important to identify the mechanisms of PCD are the dopamine neurons of the substantia nigra, the neurons which degenerate in Parkinson's disease. PCD has been shown to occur in these neurons during normal development and to be induced in neurotoxin models of parkinsonism. Conventional histologic stains and TUNEL labeling have not revealed morphologic differences in the apoptosis observed in these neurons in any context. We now show that in two models of induced PCD in postmitotic dopamine neurons, one induced by early striatal target injury and another induced by the neurotoxin 6-hydroxydopamine (6OHDA), there are differences in the cellular localization and type of caspase cleavage products. Using two antibodies to caspase cleavage products (fractin and AB127), we show that in the target lesion model immunostaining is localized to the nucleus, whereas in the 6OHDA model intense cytoplasmic as well as nuclear staining is observed. Another antibody, AB246, to a caspase cleavage product of spectrin, immunostains apoptotic profiles only in the 6OHDA model. These findings suggest that the cellular compartment and therefore the role of the caspases may differ in apoptosis induced in pathologic settings, such as that due to neurotoxins, from that observed in models of natural or induced natural cell death. It will be important to recognize these differences in the consideration of caspase inhibitors in the treatment of degenerative neurologic disease. © 2002 Elsevier

Science (USA)

Key Words: apoptosis; programmed cell death; caspase; dopamine; substantia nigra; actin; spectrin; Parkinson's disease.

INTRODUCTION

Programmed cell death (PCD) is a form of death in which genetic programs intrinsic to the cell mediate its demise (9, 17). While originally identified in neurons in the course of normal development (29), it is now recognized that PCD can occur in the adult brain in models of acute and chronic neurologic disease (36, 38). Thus, there is growing interest in the hypothesis that PCD may be an important mediator of cell death in neurodegenerative disorders such as Alzheimer's (4) and Parkinson's disease (PD) (5). In addition, it is now clear that PCD is an important regulator of viability in cell-based approaches to the treatment of some of these diseases, such as transplantation approaches to PD (21, 34).

PCD is now conceptualized to occur by three distinct, but probably interacting, pathways (24): an extrinsic pathway, which is initiated at the cell surface by the binding of ligands to death receptors (2); an intrinsic pathway, mediated by cytochrome *c* release from mitochondria (11); and an endoplasmic reticulum stress pathway (25). The intrinsic pathway is often implicated in PCD in neurons (41). PCD mediated by this pathway is initially regulated by anti- and proapoptotic members of the Bcl-2 family (1), which ultimately control the release of cytochrome *c*. Once cytochrome *c* is released, it associates with Apaf-1 and the zymogen form of caspase-9, which, in the presence of ATP, is cleaved to its active form (39). Active caspase-9 then cleaves the zymogen form of effector caspases, such as caspase-3, and activates them, enabling them to cleave cellular protein substrates.

An important emerging theme in the regulation of the intrinsic pathway in neuronal death is that the precise mechanisms involved are context and stimulus

¹ To whom correspondence should be addressed at Department of Neurology, Room 308, The William Black Medical Research Building, The College of Physicians and Surgeons, Columbia University, 650 W 168th Street, New York, NY 10032. Fax: (212) 305-5450. E-mail: rb43@columbia.edu.

dependent (42). Zaidi and co-workers have shown that while upstream regulation of the caspases by Bcl-2 family members occurs in mature neurons, it does not in neuronal precursors (33, 42). Examination of homozygous null mice has revealed that Bcl-xL deficiency does not lead to an increased incidence of apoptosis among neuronal precursors, and, on the other hand, Bax deficiency does not lead to reduced levels of apoptosis, as does caspase-3 deficiency (33).

We have had an interest in the regulation of PCD within postmitotic dopaminergic neurons of the substantia nigra (SN), the principal neurons to degenerate in PD. We have shown that natural apoptotic cell death occurs within these neurons (14, 15, 27) and that it can be induced by developmental striatal target lesion (20), medial forebrain bundle axotomy (26), or nerve terminal destruction with the neurotoxin 6-hydroxydopamine (6OHDA) (23). Conventional histologic techniques such as thionine or silver stain and TUNEL labeling do not reveal morphological differences among the apoptotic profiles observed in these models of PCD in dopamine neurons, nor do immunohistochemical stains for proteins implicated in PCD, including phosphorylated *c-jun* (28) (and unpublished observation) and *cdk5* (26). However, we have recently observed that there is a difference among these models in the cellular patterns of activation of caspase-3. In the setting of natural cell death, or that induced by early target injury, activated caspase-3 is observed strictly in a nuclear distribution (16). However, in apoptosis induced by the neurotoxin 6OHDA, activated caspase-3 is observed not only in a nuclear distribution, but also within the cytoplasm of the cell soma and neural processes (16). These observations raise the question of whether these apparent differences can be confirmed by presence of similar differences in the distribution of caspase cleavage products or by differences in cleavage substrates. To address this question we have examined by immunohistochemistry the cellular localization of caspase cleavage products using three antisera to different epitopes in two of these models of induced death: that due to striatal target injury and that induced by 6OHDA (Fig. 1). We find that apoptosis in these two models differs in the both the distribution and type of caspase cleavage products, indicating that there are distinct PCD mechanisms which can occur in postmitotic dopamine neurons.

MATERIALS AND METHODS

Animal Models

Striatal lesions with quinolinic acid (QA). Striatal QA lesions were performed as previously described (18, 20) on postnatal day (PND) 12 rats: following induction of anesthesia by hypothermia, a 28-gauge cannula was inserted into the striatum at 3.0 mm left of and 0.5 mm

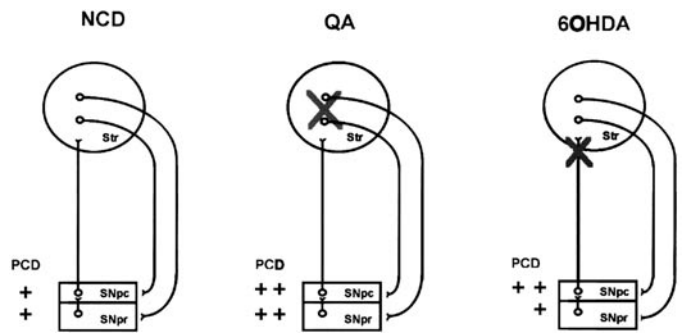


FIG. 1. Models of induced PCD in neurons of the SN. Natural cell death (NCD) occurs in neurons of both the SNpc (15, 27) and SNpr (unpublished observations). The magnitude of this death event in both regions can be induced by destruction of the striatum with the excitotoxin quinolinic acid (QA). The peak of induced death occurs at 24 h postlesion (20). Cell death can also be induced in SNpc (but not SNpr) by intrastriatal injection of 6OHDA. In this model, death is maximum between postlesion days 4 and 8 (23).

anterior to bregma, at a depth of 4.0 mm. QA (480 nmol/ μ l) in 0.1 M phosphate-buffered saline (pH 7.4) (PBS) was infused by pump at 1.0 μ l/2.0 min. This protocol has been approved by The Animal Care and Use Committee at Columbia-Presbyterian Medical Center.

6OHDA lesions. 6OHDA lesions were performed as previously described (23). PND6 rat pups were pretreated with 25 mg/kg desmethylinipramine, anesthetized by hypothermia, and placed prone on an ice pack. The skull was exposed by a midline incision, and a burr hole was placed 3.0 mm lateral to the left of bregma on the coronal suture. A 28-gauge cannula was then inserted vertically into the striatum to a depth of 4.0 mm from the top of the skull. 6OHDA hydrobromide (Regis) was prepared at 15 μ g (total weight)/1.0 μ l in 0.9% NaCl/0.02% ascorbic acid and infused by pump (Harvard Apparatus) at a rate of 0.25 μ l/min. The cannula was slowly withdrawn 2 min after the end of the infusion. After recovery from anesthesia, pups were returned to the dams until the assigned postlesion day.

Tissue Processing and Immunohistochemistry

Tissue processing. Following the QA lesion, pups were sacrificed at 24 h postlesion (PND13), and following 6OHDA, they were sacrificed at 7 days postlesion (PND13). Rat pups were anesthetized with halothane vapor, a thoracotomy was performed, and the left cardiac ventricle was cannulated with a 20-gauge needle. Each animal was then perfused with ice-cold 0.9% NaCl by gravity for 5 min. They were then perfused with ice-cold 4% paraformaldehyde/0.1 M phosphate buffer (PB) by gravity for 10 min. The brain was then carefully removed from the skull and postfixed in the same fixative for 3 h at 4°C. The brain was then cryoprotected in 20% (w/w) sucrose in 0.1 M PB for

24 h, rapidly frozen in 2-methylbutane chilled on dry ice, and sectioned through the entire SN at 20 μm on a cryostat.

Primary antibodies. The fractin antibody was raised against the last five amino acids (YELPD) of the C-terminus of the 32-kDa N-terminal fragment produced by caspase cleavage between Asp244 and Gly245 of actin during apoptosis (40). This antiserum does not recognize full-length actin, but does detect a 32-kDa polypeptide generated by incubation of actin with a caspase-3 extract from apoptotic cells (40). In tissue culture, the induction of fractin-generating activity closely parallels that of caspase-3-like activity, and it is inhibited by specific inhibitors of caspase-3-like activity. We have previously shown that in brain sections, positive fractin staining is exclusively observed in cells with apoptotic nuclear chromatin clumps (14). For these studies, we have used the fractin antibody at a dilution of 1:100. The fractin antibody was a kind gift of Drs. G. Cole and F. Yang, UCLA. AB127 was raised against a predicted caspase cleavage sequence within poly(ADP-ribose) polymerase (PARP), KGDEVD, at the C-terminus of the N-terminal fragment (35). AB127 detects a 46-kDa polypeptide which appears and increases with time in preparations of PC12 cells undergoing apoptosis following NGF withdrawal. It also detects a 46-kDa polypeptide which can be generated by treatment of PC12 extracts with recombinant caspase-3 protein. Both *in vitro* and *in vivo*, AB127 immunoreactivity appears exclusively in association with apoptotic nuclear morphology (10, 35). For these studies AB127 was used at a dilution of 1:2500.

AB246 was raised against a predicted caspase cleavage sequence within α -spectrin, GPRDET, at the C-terminus of the 156-kDa N-terminal fragment. The specificity of AB246 was evaluated by immunoblot analysis of SY5Y human neuroblastoma cells degenerating in response to three mechanistically distinct proapoptotic stimuli. SY5Y cells were grown in 35-mm dishes to near confluency and then treated with either fresh serum-containing growth medium (control, no addition), staurosporine (300 nM, 6 h), tunicamycin (2 $\mu\text{g}/\text{ml}$, 24 h), or growth-factor-deficient medium (serum-free + LY294002, 50 μM , 24 h). Following two washes, cells were harvested in 75 μl /well SDS-PAGE running buffer, and polypeptides were separated by SDS-PAGE and transferred to a PVDF membrane. The membrane was immunostained with AB246 at 1:3000 using enhanced chemiluminescence. Whereas AB246 exhibited little labeling of control cells, apoptotic SY5Y extracts contained an immunoreactive polypeptide of ~ 150 kDa, which is the predicted size of the caspase-derived N-terminal fragment of α -spectrin (Fig. 2). AB246 also exhibits detectable but less intense labeling of an ~ 75 -kDa polypeptide induced by staurosporine treatment that is of unknown origin. AB246

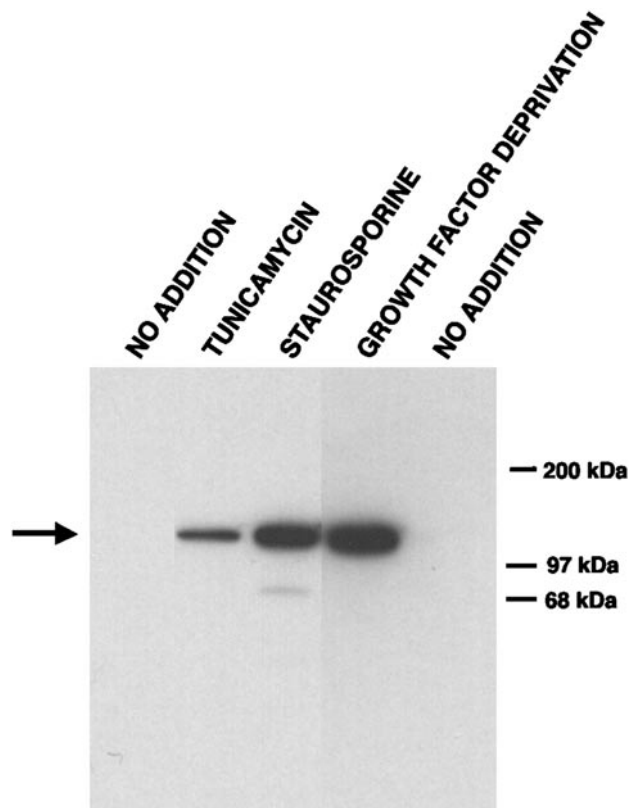


FIG. 2. Specificity of AB246 for a caspase-derived fragment of α -spectrin. SY5Y human neuroblastoma cells were either maintained in growth medium (no addition) or treated with the indicated proapoptotic stimuli, as described under Materials and Methods. Immunoblot analysis demonstrates that in healthy cells AB246 does not react with intact α -spectrin (~ 250 kDa) or any other polypeptide. In apoptotic extracts, in contrast, AB246 intensely stains the caspase-derived ~ 150 kDa N-terminal fragment of α -spectrin.

does not react with the ~ 150 - or ~ 145 -kDa derivatives of α -spectrin produced by calpain cleavage (data not shown). These reactivities are blocked when cells are treated with a caspase inhibitor. By immunocytochemistry, AB246 has been shown to react preferentially with apoptotic but neither healthy nor necrotic neurons in cell culture (R. Siman, submitted for publication). AB246 was used at a dilution of 1:1000.

Immunoperoxidase staining. For all protocols, sections were collected into PBS and processed free floating. After washes in PBS, sections were pretreated with PBS/0.5% BSA and then incubated in primary antibody in this solution for 48 h at 4 $^{\circ}$ C. Sections were then treated with biotinylated protein A (prepared in our laboratory) at 1:100 for 60 min at room temperature. Following additional washes, sections were incubated with avidin-biotin-horseradish peroxidase complexes (ABC, Vector Labs) at 1:600 for 60 min at room temperature. Following washes in PBS, sections were incubated in a solution of diaminobenzidine (50 mg in 100 ml Tris buffer, pH 7.6) containing glucose oxidase,

ammonium chloride and D(+)-glucose to generate H_2O_2 .

Immunofluorescence double labeling. Brains were postfixed for 3 h. Sections were cut at 20 μm and then incubated with PBS/0.1% Triton/10% goat serum/10% horse serum. They were then incubated with anti-TH (1:40) (Chemicon) or anti-fractin (1:100) or both for 48 h at 4°C. Following washes, they were incubated with Texas-red-conjugated horse anti-mouse at 1:75 and fluorescein-conjugated goat anti-rabbit at 1:75 in TBS-T/10% goat serum/10% horse serum for 1 h. Sections were then stained with Hoechst 33342 (Molecular Probes) at 1:500 to visualize apoptotic chromatin clumps. Sections were coverslipped with Dako antifade medium and viewed with appropriate filters by epifluorescence on a Nikon Eclipse 800 microscope. Images were captured with a Spot II digital camera and single channel images were merged using Adobe Photoshop.

Qualitative morphologic analysis. In the immunoperoxidase-stained material, apoptosis was identified at the light microscope level by performing a thionine counterstain and visualizing intranuclear chromatin clumps as one or more intensely basophilic, homogeneously stained, round, and distinctly bounded structures. We have previously shown for both the striatal lesion and the 6OHDA models that apoptotic profiles so identified are confirmed to be apoptotic by electron microscopy (20; and unpublished observations). Profiles so identified can also be confirmed as apoptotic by TUNEL labeling and suppressed silver staining (20, 23). In the immunofluorescence double-labeled material, apoptotic profiles were identified by the presence of intensely fluorescent, round, and distinctly bounded structures within the nucleus on UV illumination.

Quantitative morphologic analysis. For analysis of the QA model, sections from three animals were processed for immunostaining with each of the three antibodies; for the 6OHDA model, sections from four animals were processed. To determine the percentage of apoptotic profiles in the SN immunostained for each immunogen, all available sections for each animal were scanned at 600 \times and all apoptotic profiles identified by the above criteria were counted. For each apoptotic profile, it was determined whether there was positive immunostaining. In no instance was there positive immunostaining in the absence of apoptotic chromatin clumps. Sections were processed free floating, and nonserially, but for each brain there were sections representative of each of the major SN planes, identified in the Paxinos–Watson atlas as planes 4.2, 3.7, and 3.2 (32). Because the number of sections available for each animal varied, so also did the absolute number of apoptotic profiles (Table 1). Thus, the absolute number of sampled apoptotic profiles for each immunogen does not meaningfully reflect the magnitude of induced death in different animals or models. However, there

TABLE 1

Apoptotic Profiles Sampled in Sections Immunostained for Caspase Cleavage Products

Model	Antibody	N (rats)	Sections	Apoptotic profiles	Profiles per section
QA	Fractin	3	22	86	3.91
QA	AB127	3	30	139	4.63
QA	AB246	3	26	162	6.23
6OHDA	Fractin	4	44	207	4.70
6OHDA	AB127	4	39	199	5.10
6OHDA	AB246	4	39	159	4.08

was no difference between the two models in mean number of apoptotic profiles per section (QA, 4.9 ± 0.7 ; 6OHDA, 4.6 ± 0.3 , NS).

RESULTS

Immunostaining of SN sections with the fractin and AB127 antibodies in the target injury model revealed positive staining of apoptotic profiles in a nuclear distribution (Fig. 3). Staining was always observed in a small ($\sim 5.0 \mu m$), circular pattern surrounding apoptotic chromatin clumps, identified by thionine counterstain. Staining was never observed within the cytoplasm of cells in this model. This pattern of staining is identical to that which we previously reported for the activated form of caspase-3 in the target injury model (16).

Staining with these antibodies was not observed in all apoptotic profiles in SN. For fractin, positive staining was observed in 24 of 86 (28%) of profiles examined among $N = 3$ animals. AB127 staining was observed in a smaller percentage; only 8 of 139 (6%) of profiles were stained. These percentages are substantially lower than that observed for activated caspase-3, which we reported as 59% in this model (16).

In the target injury model, efforts to demonstrate caspase cleavage of spectrin with the AB246 antibody failed to reveal positive profiles, in spite of a clear demonstration of staining in the 6OHDA model, as presented below, processed in parallel. A total of 162 apoptotic profiles in the SNpc were examined in $N = 3$ animals. One revealed possible positive staining, but in the absence of other confirmatory profiles, it could not be certain that this was authentic.

Caspase cleavage products were also detected by immunostaining in the 6OHDA model. As predicted on the basis of activated caspase-3 staining in this model (16), the staining was not only nuclear, as observed in the target injury model, but also cytoplasmic (Fig. 4). In the example of positive fractin staining shown in Fig. 4A, the cytoplasmic staining was more pronounced than the nuclear staining. In other profiles, approximately equal levels of staining could be observed in the

two cellular compartments. A similar pattern of staining was observed with the AB127 antibody, as shown in Fig. 4B.

Similar to the target injury model, not all apoptotic profiles were positive for either fractin or AB127. Among 207 apoptotic profiles in the SNpc in $N = 4$ animals lesioned with 6OHDA, 28 (14%) were fractin positive. Of these 15 (or 7%) showed only nuclear staining; the remaining 13 (6%) showed cytoplasmic staining in the presence or absence of nuclear staining. Among 199 profiles examined in $N = 4$ animals, 29 (15%) were positive for AB127 staining. Unlike the fractin staining, however, a very small number (only 2) showed only nuclear staining; the large majority (27, or 99%) showed cytoplasmic staining in the presence or absence of nuclear staining. The total percentages of profiles stained with these antibodies, 14 and 15% for fractin and AB127, respectively, is quite similar to the 15% we had previously reported for the number of caspase-3-positive profiles in the 6OHDA model (16).

Unlike the target injury model, the 6OHDA model induced the expression of caspase cleavage products of spectrin (Fig. 4C). As for fractin and AB127 immunostaining, AB246 staining was observed in both the nucleus and the cytoplasm. The profile demonstrated in Fig. 4C is one in which the nuclear and cytoplasmic peroxidase staining are equally apparent. A similar percentage of profiles was stained, compared to fractin and AB127 (23 of 159, 14%). As for AB127 staining, the large majority of profiles showed cytoplasmic staining (20 of 23, or 87%).

While we have previously shown that induced apoptotic death in both the target injury and the 6OHDA models occurs in phenotypically defined dopamine neurons, we have not shown, for either model, that it occurs exclusively in these neurons. It is therefore theoretically possible that the differences in morphology and patterns of protein cleavage which we have observed in these two models could be attributed to differences in the cellular phenotype of the stained profiles. To address this issue, we determined the pattern of staining in defined dopamine neurons by use of immunofluorescence double labeling for fractin and tyrosine hydroxylase. In the target injury model, double labeling confirmed that when positive fractin staining is identified within apoptotic dopaminergic neurons, it is exclusively expressed within the nucleus (Fig. 5). In the 6OHDA model, when fractin staining is identified within apoptotic dopaminergic neurons, it is present in the cytoplasm alone (Figs. 6A–6D), in both the cytoplasm and the nucleus (Figs. 6E–6H), or in the nucleus alone (not shown). Thus, the differences in cellular morphology of caspase cleavage products that we have identified in these two models can be observed within defined dopamine neurons and are not due to differences in cell phenotype.

DISCUSSION

It has been recognized for some time that different cell phenotypes utilize different pathways of PCD. While cell death by the extrinsic pathway has frequently been implicated in the death of lymphocytes, cancer cells and inflammatory cells (2), the intrinsic pathway has more often been implicated in death of cells in the nervous system (41). However, it has become apparent only more recently that even within neurons, regulation of the intrinsic pathway differs depending on the stimulus and context. Zaidi and co-investigators have shown that the Bcl-2 family of apoptosis regulators appear to play a role in controlling caspase activation in the intrinsic pathway predominantly in postmitotic neurons and not in neuronal precursors (33, 42). The general concept that the involvement of specific death molecules may be dependent on specific brain region and maturity is reinforced for the caspases by the recent observation that although caspase-3 and caspase-9 homozygous null mutations lead to striking forebrain morphologic abnormalities, the spinal cord and brain stem appear normal (30). Aside from any differences in death pathways that may be due to differences in brain region, cell phenotype, or age, it is also clear from studies in tissue culture that differences may also arise from the nature of the death stimulus. Park and colleagues have shown that PCD in postmitotic sympathetic neurons in culture differs in its regulation by cyclin-dependent protein kinases and its mediation by caspases, depending on whether it is induced by trophic factor withdrawal, DNA damage, or oxidative stress (31).

It has been unknown whether different mechanisms of PCD might occur in postmitotic dopamine neurons of the SN *in vivo*. Apoptosis has been unequivocally identified in these neurons during normal development (14, 15, 27) and shown to occur in models of disease induced by the neurotoxins 6OHDA (13, 23) and MPTP (37), in both immature and adult animals. Apoptosis has not previously been demonstrated to have different morphologies or mechanisms in these diverse contexts. No differences in morphology have been identified on routine histologic stains or by TUNEL labeling. In the case of apoptosis induced by intrastriatal injection of 6OHDA, we had previously hypothesized that the increased level of death was due to destruction of dopamine terminals, an inability to take up target-derived trophic support, and a resulting induction of ongoing natural cell death, as envisioned by classic neurotrophic theory (3, 6). On the basis of this hypothesis, and in view of the identical morphology of apoptosis by conventional techniques in the 6OHDA and the striatal target injury models, it seemed most parsimonious to propose that identical mechanisms of PCD were operative.

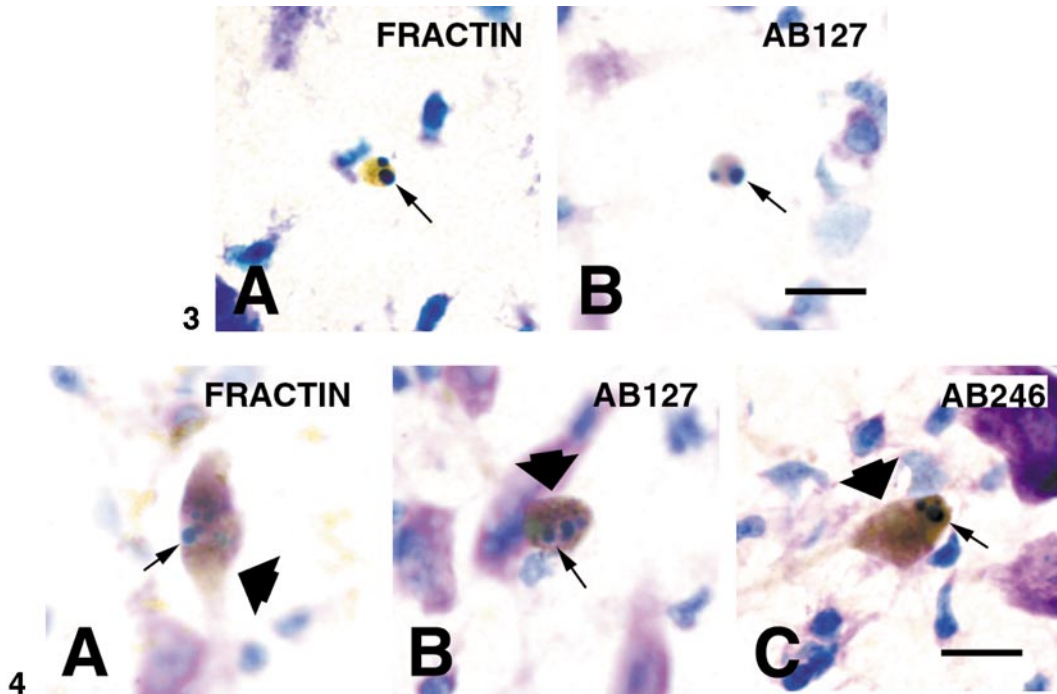


FIG. 3. Fractin and AB127 immunostaining in the SNpc in the QA striatal target injury model. (A) A fractin-positive immunoperoxidase stained profile (brown chromagen) is observed in the SNpc at 24 h following striatal QA lesion of a PND12 rat. Two blue thionine-stained apoptotic chromatin clumps (one is indicated by an arrow) are observed within the peroxidase-stained nucleus. (B) An AB127-positive profile is observed within the SNpc at 24 h postlesion. Two apoptotic chromatin clumps are observed (one is indicated by an arrow). Bar 10 μm .

FIG. 4. Fractin, AB127 and AB246 staining in the SNpc in the 6OHDA injury model. (A) A fractin-positive immunoperoxidase-stained profile is observed in SNpc at 7 days following a lesion on PND6. Multiple, rounded, blue thionine-stained apoptotic chromatin clumps are observed within the nucleus of this neuron (one is indicated by a thin black arrow). The most intense brown peroxidase stain is observed in the cytoplasm of this neuron (wide black arrow). (B) An AB127-positive profile is observed in SNpc at 7 days postlesion. Multiple apoptotic chromatin clumps are within the nucleus. The most intense peroxidase staining is outside of the nucleus, in the cytoplasm (wide black arrow). (C) In this profile, AB246 staining is observed both in the nucleus, surrounding the apoptotic chromatin clumps (narrow black arrow), and in the cytoplasm (wide arrow). Bar 10 μm .

However, two observations do not conform to this concept. First, the developmental time course for the QA and the 6OHDA models is not the same. In the QA target injury model, there is virtually no induction of death after PND14 (18), whereas in the 6OHDA model, while the level of induction is much less after PND14, it nevertheless occurs, even as late as 7 weeks of age (23). Second, as previously noted, the cellular distribution of activated caspase-3 differs between the two models. In the QA model, activated caspase-3 is demonstrable only in the nucleus, whereas in the 6OHDA model, it is identified in the cytoplasm as well. The present results confirm and extend these observations by demonstrating that a similar difference between the two models exists for the cellular distribution of two caspase cleavage products. In addition a caspase cleavage product of spectrin is demonstrable only in the 6OHDA model, and it too is identified in the cytoplasm.

We interpret these differences in the patterns of cellular morphology and protein cleavage between the two models to be due to differences in functional caspase activity in different cell compartments *in vivo*. While immunostaining of activated caspase-3 can ap-

parently occur as a postmortem artifact (12), we doubt that such an effect could account for the differences we have observed. In our previous study of activated caspase-3 staining, we never observed staining in the absence of colocalized nuclear apoptotic chromatin clumps. In addition, a transient postmortem cleavage of caspase-3 seems unlikely to result in extensive cleavage of protein substrates, such as we have observed. Furthermore, in the present study, the staining of caspase cleavage products, like activated caspase-3, was always observed in association with apoptotic chromatin morphology.

The differences we have observed cannot be attributed to age, relationship to the cell cycle or cell phenotype. Animals in the two models were studied at the same age, all dopamine neurons are postmitotic at this postnatal age (8, 19, 22), and these morphologic differences were demonstrated in the two models for defined dopamine neurons.

We also observed a difference in the two models in terms of the relative abundance of caspase cleavage products. In the target injury model we observed relatively fewer cleavage product-positive profiles in com-

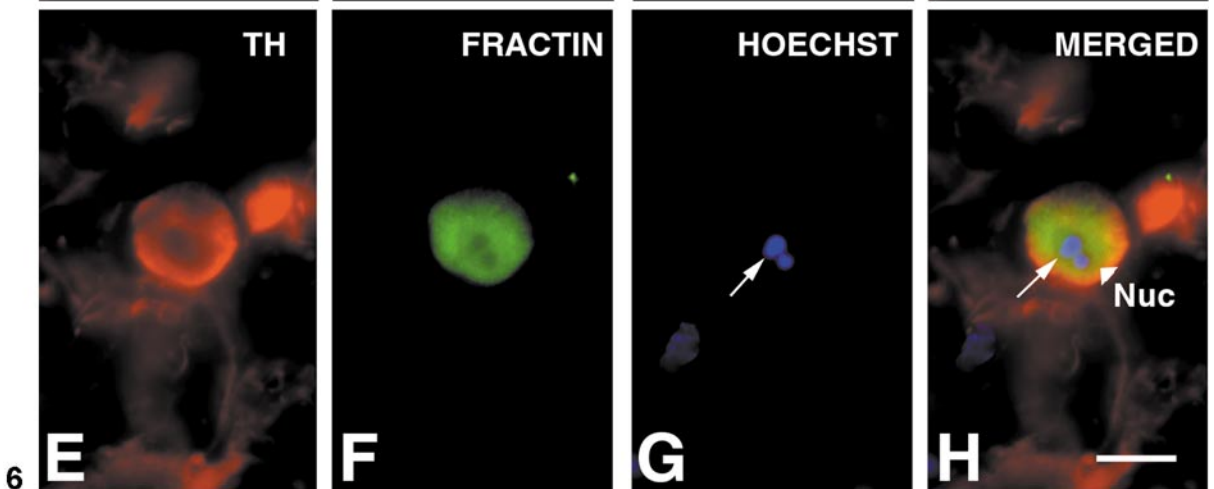
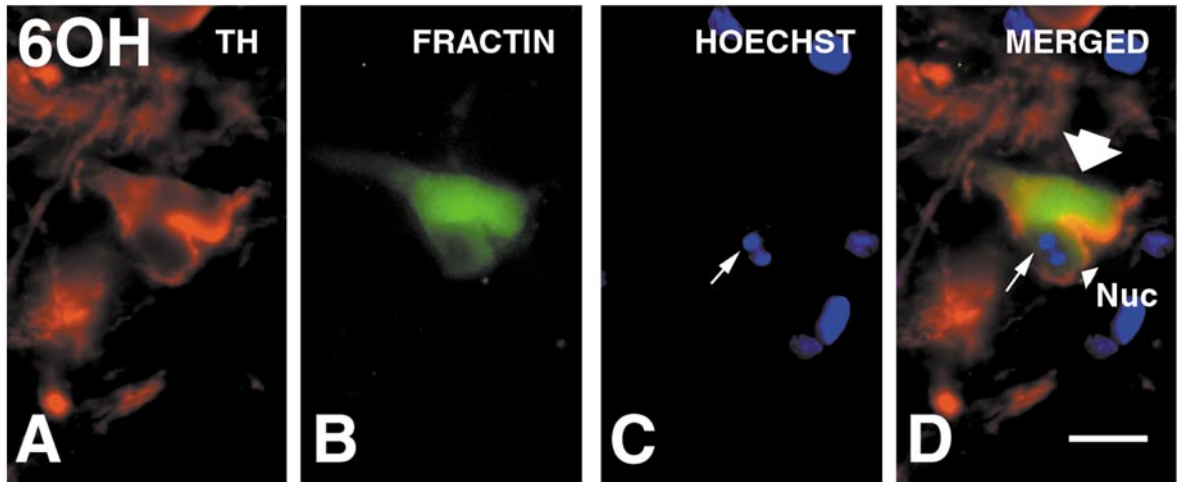
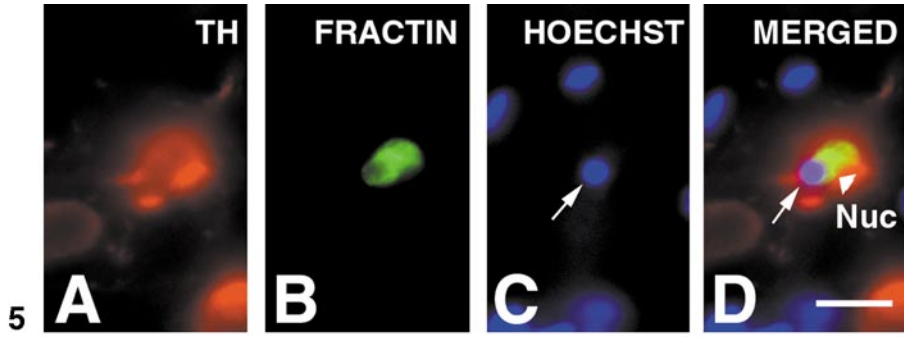


FIG. 5. Double immunofluorescence labeling with fractin and an antibody to tyrosine hydroxylase (TH) in the SNpc following striatal lesion with QA. (A) The dopamine phenotype of this neuron has been demonstrated by Texas red staining for TH. (B) The presence of fractin staining in the nucleus is shown by green fluorescein staining. (C) An apoptotic chromatin clump within the nucleus is indicated by staining with Hoechst 33342 and UV illumination. (D) A merged image demonstrating colocalization of fractin and TH in this apoptotic profile. The localization of the fractin stain to the central nuclear (Nuc; arrowhead) region, which is relatively devoid of TH staining, is apparent. Other double-labeled profiles showed a similar pattern. In the target injury model, fractin labeling in TH-positive neurons was always restricted to the nucleus. Bar 10 μm .

FIG. 6. Double immunofluorescence labeling with fractin and an antibody to tyrosine hydroxylase (TH) in the SNpc following lesion with 60HDA (60H). In the profile depicted in (A–D), the dopaminergic phenotype is demonstrated by TH staining (Texas red) (A), fractin staining by fluorescein (B), and apoptotic chromatin by Hoechst 33342 (C). (D) The merged image demonstrates that the most intense fractin staining is in the cytoplasm; the nucleus (Nuc; arrowhead) is relatively devoid of staining. In E–H, a second TH-positive profile is shown in which fractin staining is present both in the cytoplasm and the nucleus (Nuc, arrowhead). Bar 10 μm .

parison to the numbers of activated caspase-3-positive profiles, which we previously reported to be 59% (16). In the 6OHDA model, the proportion of apoptotic profiles positive for caspase cleavage products was about the same as what we had reported for caspase-3-positive profiles, which was 15% (16). One interpretation of these results is that for a given level of caspase-3 activity, there is more substrate cleavage in the 6OHDA model. Alternatively, these differences may be due to differences in the cellular compartments in which caspase-3 is active in the two models. In the 6OHDA model, the presence of activated caspase-3 in the cytoplasm may result in more readily stainable cleavage products by immunohistochemistry compared to the target injury model, where the cleavage products are strictly nuclear, and less accessible to staining by immunoreagents.

The localization of activated caspase-3 and the caspase cleavage product of actin recognized by the fractin antibody to the nucleus in the target injury model is identical to what we have previously described for natural cell death in SNpc neurons in rat (16) and mouse (14). It thus seems possible that the induction of death in dopamine neurons following striatal target injury represents an augmentation of natural cell death, as proposed in classic neurotrophic theory (3), and cell death mechanisms in these two settings are similar. In 6OHDA-induced death, however, the appearance of activated caspase-3 and cleavage products in the cytoplasm is unlike what we have observed in natural cell death. This ectopic activation of caspases in the cytoplasm may occur in other neurotoxin models of apoptotic dopamine neuron death. Eberhardt and colleagues have shown that in the adult MPTP model of apoptotic dopamine neuron death, activated caspase-3 is identified predominantly in the cytoplasm (7).

These findings have functional implications for the possible role of caspases in pathologic states of apoptotic cell death. Oppenheim and co-investigators have recently shown that in caspase-3 and caspase-9 null mice there is no decrease in the number of neurons which die by natural cell death in spinal and brainstem motor nuclei, spinal interneurons, dorsal root, or sympathetic ganglia (30). Furthermore, when natural neuron death occurs in these mutants, cytoplasmic degenerative changes are observed, but nuclear changes and TUNEL labeling are diminished. These findings suggest that for some neuronal populations, for natural cell death, caspases are not essential, and they seem to primarily mediate nuclear change, a late apoptotic event. If such were the only role for the caspases, then their inhibition by pharmacologic antagonists would offer little therapeutic benefit in the treatment of degenerative neurologic disease. However, our results show that in a pathologic setting, that of apoptosis induced by neurotoxins, the role of caspases may be quite different. In this setting, they are active in the

cytoplasm. Our studies do not permit an analysis of the time course of their activation, but it is conceivable that in this setting, their activation in the cytoplasm may be an earlier event than the nuclear events mediated by caspases in natural cell death. Thus, in pathologic apoptosis, such as may occur in disease, it may remain a worthwhile therapeutic goal to inhibit caspase-mediated cytoplasmic proteolysis.

ACKNOWLEDGMENTS

We are indebted to Drs. Greg Cole and Fusheng Yang for sharing their fractin antibody. This work was supported by NS26836 and NS38370, The Parkinson's Disease Foundation, and the Lowenstein Foundation.

REFERENCES

1. Adams, J. M., and S. Cory. 1998. The Bcl-2 protein family: Arbiters of cell survival. *Science* **281**: 1322–1326.
2. Ashkenazi, A., and V. M. Dixit. 1998. Death receptors: Signaling and modulation. *Science* **281**: 1305–1308.
3. Barde, Y. A. 1989. Trophic factors and neuronal survival. *Neuron* **2**: 1525–1534.
4. Barinaga, M. 1998. Is apoptosis key in Alzheimer's disease? *Science* **281**: 1303–1304.
5. Burke, R. E., and N. G. Kholodilov. 1998. Programmed cell death: Does it play a role in Parkinson's disease? *Ann. Neurol.* **44**: S126–S133.
6. Clarke, P. G. H. 1985. Neuronal death in the development of the vertebrate nervous system. *Trends Neurosci* **8**: 345–349.
7. Eberhardt, O., R. V. Coelln, S. Kugler, J. Lindenau, S. Rathke-Hartlieb, E. Gerhardt, S. Haid, S. Isenmann, C. Gravel, A. Srinivasan, M. Bahr, M. Weller, J. Dichgans, and J. B. Schulz. 2000. Protection by synergistic effects of adenovirus-mediated Xchromosome-linked inhibitor of apoptosis and glial cell line-derived neurotrophic factor gene transfer in the 1-methyl-4-phenyl-1,2,3,6-tetrahydropyridine model of Parkinson's disease. *J. Neurosci.* **20**: 9126–9134.
8. El-Khodori, B. F., N. Kholodilov, O. Yarygina, and R. E. Burke. 2001. The expression of mRNAs for the proteasome complex is developmentally regulated in the rat mesencephalon. *Dev. Brain Res.* **129**: 47–56.
9. Ellis, R. E., J. Yuan, and H. R. Horvitz. 1991. Mechanisms and functions of cell death. *Ann. Rev. Cell Biol.* **7**: 663–698.
10. Finn, J. T., M. Weil, F. Archer, R. Siman, A. Srinivasan, and M. C. Raff. 2000. Evidence that Wallerian degeneration and localized axon degeneration induced by local neurotrophin deprivation do not involve caspases. *J. Neurosci.* **20**: 1333–1341.
11. Green, D. R., and J. C. Reed. 1998. Mitochondria and apoptosis. *Science* **281**: 1309–1312.
12. Hartmann, A., S. Hunot, P. P. Michel, M. P. Muriel, S. Vyas, B. A. Faucheux, A. Mouatt-Prigent, H. Turmel, A. Srinivasan, M. Ruberg, G. I. Evan, Y. Agid, and E. C. Hirsch. 2000. Caspase-3: A vulnerability factor and final effector in apoptotic death of dopaminergic neurons in Parkinson's disease. *Proc. Natl. Acad. Sci. USA* **97**: 2875–2880.
13. He, Y., T. Lee, and S. K. Leong. 2000. 6-Hydroxydopamine induced apoptosis of dopaminergic cells in the rat substantia nigra. *Brain Res.* **858**: 163–166.
14. Jackson-Lewis, V., M. Vila, R. Djaldetti, C. Guegan, G. Liberatore, J. Liu, K. L. O'Malley, R. E. Burke, and S. Przedborski. 2000. Developmental cell death in dopaminergic neurons of the substantia nigra of mice. *J. Comp. Neurol.* **424**: 476–488.

15. Janec, E., and R. E. Burke. 1993. Naturally occurring cell death during postnatal development of the substantia nigra of the rat. *Mol. Cell. Neurosci.* **4**: 30–35.
16. Jeon, B. S., N. G. Kholodilov, T. F. Oo, S. Kim, K. J. Tomaselli, A. Srinivasan, L. Stefanis, and R. E. Burke. 1999. Activation of caspase-3 in developmental models of programmed cell death in neurons of the substantia nigra. *J. Neurochem.* **73**: 322–333.
17. Johnson, E. M., and T. L. Deckwerth. 1993. Molecular mechanisms of developmental neuronal death. *Annu. Rev. Neurosci.* **16**: 31–46.
18. Kelly, W. J., and R. E. Burke. 1996. Apoptotic neuron death in rat substantia nigra induced by striatal excitotoxic injury is developmentally dependent. *Neurosci. Lett.* **220**: 85–88.
19. Lauder, J. M., and F. E. Bloom. 1974. Ontogeny of monoamine neurons in the locus coeruleus, raphe nuclei and substantia nigra of the rat. *J. Comp. Neurol.* **155**: 469–482.
20. Macaya, A., F. Munell, R. M. Gubits, and R. E. Burke. 1994. Apoptosis in substantia nigra following developmental striatal excitotoxic injury. *Proc. Natl. Acad. Sci. USA* **91**: 8117–8121.
21. Mahalik, T. J., W. E. Hahn, G. H. Clayton, and G. P. Owens. 1994. Programmed cell death in developing grafts of fetal substantia nigra. *Exp. Neurol.* **129**: 27–36.
22. Marchand, R., and L. J. Poirer. 1983. Isthmic origin of neurons of the rat substantia nigra. *Neuroscience* **9**: 373–381.
23. Marti, M. J., C. J. James, T. F. Oo, W. J. Kelly, and R. E. Burke. 1997. Early developmental destruction of terminals in the striatal target induces apoptosis in dopamine neurons of the substantia nigra. *J. Neurosci.* **17**: 2030–2039.
24. Mehmet, H. 2000. Caspases find a new place to hide [news]. *Nature* **403**: 29–30.
25. Nakagawa, T., H. Zhu, N. Morishima, E. Li, J. Xu, B. A. Yankner, and J. Yuan. 2000. Caspase-12 mediates endoplasmic-reticulum-specific apoptosis and cytotoxicity by amyloid-beta. *Nature* **403**: 98–103.
26. Neystat, M., M. Rzhetskaya, T. F. Oo, N. Kholodilov, O. Yarygina, A. Wilson, B. F. El-Khodori, and R. E. Burke. 2001. Expression of cyclin-dependent kinase 5 and its activator p35 in models of induced apoptotic death in neurons of the substantia nigra in vivo. *J. Neurochem.* **77**: 1611–1625.
27. Oo, T. F., and R. E. Burke. 1997. The time course of developmental cell death in phenotypically defined dopaminergic neurons of the substantia nigra. *Dev. Brain Res.* **98**: 191–196.
28. Oo, T. F., C. Henchcliffe, D. James, and R. E. Burke. 1999. Expression of c-fos, c-jun, and c-jun N-terminal kinase (JNK) in a developmental model of induced apoptotic death in neurons of the substantia nigra. *J. Neurochem.* **72**: 557–564.
29. Oppenheim, R. W. 1991. Cell death during development of the nervous system. *Annu. Rev. Neurosci.* **14**: 453–501.
30. Oppenheim, R. W., R. A. Flavell, S. Vinsant, D. Prevette, C. Y. Kuan, and P. Rakic. 2001. Programmed cell death of developing mammalian neurons after genetic deletion of caspases. *J. Neurosci.* **21**: 4752–4760.
31. Park, D. S., E. J. Morris, L. Stefanis, C. M. Troy, M. L. Shelanski, H. M. Geller, and L. A. Greene. 1998. Multiple pathways of neuronal death induced by DNA damaging agents, NGF deprivation, and oxidative stress. *J. Neurosci.* **18**: 830–840.
32. Paxinos, G., and C. Watson. 1982. *The Rat Brain in Stereotaxic Coordinates*, Academic Press, San Diego, CA.
33. Roth, K. A., C. Kuan, T. F. Haydar, C. D'Sa-Eipper, K. S. Shindler, T. S. Zheng, K. Kuida, R. A. Flavell, and P. Rakic. 2000. Epistatic and independent functions of caspase-3 and Bcl-X(L) in developmental programmed cell death. *Proc. Natl. Acad. Sci. USA* **97**: 466–471.
34. Schierle, G. S., O. Hansson, M. Leist, P. Nicotera, H. Widner, and P. Brundin. 1999. Caspase inhibition reduces apoptosis and increases survival of nigral transplants. *Nature Med.* **5**: 97–100.
35. Siman, R., D. Bozyczko-Coyne, S. L. Meyer, and R. V. Bhat. 1999. Immunolocalization of caspase proteolysis in situ: Evidence for widespread caspase-mediated apoptosis of neurons and glia in the postnatal rat brain. *Neuroscience* **92**: 1425–1445.
36. Stefanis, L., R. E. Burke, and L. A. Greene. 1997. Apoptosis in neurodegenerative disorders. *Curr. Opin. Neurol.* **10**: 299–305.
37. Tatton, N. A., and S. J. Kish. 1997. In situ detection of apoptotic nuclei in the substantia nigra compacta of 1-methyl-4-phenyl-1,2,3,6-tetrahydropyridine-treated mice using terminal deoxynucleotidyl transferase labelling and acridine orange. *Neuroscience* **77**: 1037–1048.
38. Thompson, C. B. 1995. Apoptosis in the pathogenesis and treatment of disease. *Science* **267**: 1456–1462.
39. Thornberry, N. A., and Y. Lazebnik. 1998. Caspases: Enemies within. *Science* **281**: 1312–1316.
40. Yang, F., X. Sun, W. Beech, B. Teter, S. Wu, J. Sigel, H. V. Vinters, S. A. Frautschy, and G. M. Cole. 1998. Antibody to caspase-cleaved actin detects apoptosis in differentiated neuroblastoma and plaque-associated neurons and microglia in Alzheimer's disease. *Am. J. Pathol.* **152**: 379–389.
41. Yuan, J., and B. A. Yankner. 2000. Apoptosis in the nervous system. *Nature* **407**: 802–809.
42. Zaidi, A. U., C. D'Sa-Eipper, J. Brenner, K. Kuida, T. S. Zheng, R. A. Flavell, P. Rakic, and K. A. Roth. 2001. Bcl-X(L)-caspase-9 interactions in the developing nervous system: evidence for multiple death pathways. *J. Neurosci.* **21**: 169–175.